Available online at **www.joac.info**

ISSN: 2278-1862

Journal of Applicable Chemistry

2013, 2 (5):1296-1314

(International Peer Reviewed Journal)

Synthesis Of New Benzimidazole Derivatives And Their Corrosion Inhibition Performance On Mild Steel In 0.5 M Hydrochloric Acid

Doddahosuru M. Gurudatt and Kikkeri N. Mohana*

*Department of Studies in Chemistry, University of Mysore, Manasagangothri, Mysore 570 006, Karnataka, **INDIA**

Email: drknmohana@gmail.com, shivamma.guru@gmail.com

Received on 5th September and finalized on 11th September 2013.

ABSTRACT

The influence of three newly synthesized benzimidazole derivatives on the corrosion inhibition of mild steel in 0.5 M HCl solution is studied using mass loss and electrochemical techniques. The corrosion rate was found to be depends on concentration and temperature of the medium. Adsorption of all the three inhibitors obeys Langmuir isotherm model. Polarization curves indicated that the studied inhibitors are of mixed type. Electrochemical impedance spectroscopy explains the mechanism of inhibitor's action. Various activation and adsorption thermodynamic parameters were calculated and discussed. The results obtained from weight loss and electrochemical studies are in good agreement with each other. The variation in inhibitive efficiency mainly depends on the type and nature of the substituents present in the inhibitor molecule.

Keywords: Mild Steel, Acid inhibition, Weight loss, Polarization, EIS.

INTRODUCTION

Mild steel is widely applied as constructional material in many chemical and petrochemical industries due to its excellent mechanical properties and low cost. The major disadvantage is that, it is prone to undergo corrosion on exposure to corrosive environment [1, 2]. Hydrochloric acid solutions are widely used in several industrial processes such as acid pickling, acid cleaning, and acid descaling [3, 4]. Pickling involves the chemical removal of oxides and scale from the surface of strip, sheet, plate, or semi-finished products of iron and steel with an aqueous solution of inorganic acid such as sulphuric or hydrochloric acid. Hydrochloric acid pickling is faster and cleaner, consumes less acid, and produces reduced quantities of waste pickle liquor. Because of the aggressiveness of acid solutions, mild steel corrodes severely during these processes, which results in terrible waste of both resources and money [5]. Corrosion inhibitors are of great practical importance, being extensively employed in minimizing the metallic waste in engineering materials [6].

Corrosion inhibitors are often added to mitigate the corrosion of metal by acid attack. Most well-known corrosion inhibitors are organic compounds containing polar groups including nitrogen, sulphur, and/or oxygen atoms and conjugated double bonds [7-9]. These compounds can adsorb on the metal surface and block the active sites on the surface, thereby reducing the corrosion rate. Most investigations of corrosion inhibition have been related to the application of common inhibitors such as derivatives of pyrazole [10,

11], triazole [12, 13], tetrazole [14, 15], imidazole [16] and bipyrazole [17] as potential corrosion inhibitors for mild steel in acid solutions. Among various acid organic inhibitors, N-heterocyclic compounds have received a considerable amount of attention. Up to now, many N heterocyclic compounds with one or several N-heteroatoms have been investigated as corrosion inhibitors for mild steel in HCl and H_2SO_4 solutions [18-21]. It is generally accepted that N-heterocyclic compounds exert their inhibition by adsorption on the metal surface through N atom as well as those with triple or conjugated double bonds or aromatic rings in their molecular structures. Furthermore, corrosion inhibition efficiency of N-heterocyclic compounds increases with the increase of the number of aromatic systems and the availability of electronegative atoms in the molecule [22, 23].

Benzimidazole molecule shows two anchoring sites suitable for surface bonding. 1, 3 Nitrogen atoms with its lone pair of electron and the aromatic rings facilitate the adsorption of compounds on the metallic surface [24]. Benzimidazole and its derivatives have received widespread research as excellent inhibitors for mild steel and its alloys in acidic solution [25-28] for their characteristic structure, high inhibition performance, low mammalian toxicity and biodegradation. In view of its excellent behaviour as efficient corrosion inhibitor, the present work intended to synthesize three benzimidazole derivatives and investigate their efficiency as corrosion inhibitors for mild steel in 0.5 M hydrochloric acidic solution using mass loss and electrochemical techniques. The experimental findings were discussed with various activation and adsorption thermodynamic parameters. The protective film formed on the metal surface was characterized by SEM. Inhibition mechanism of benzimidazole derivatives has been proposed.

MATERIALS AND METHODS

Materials and sample preparation: Mild steel (MS) specimens used in the present study having the following chemical composition (in wt %): C - 0.051; Mn - 0.179; Si - 0.006; P - 0.005; S - 0.023; Cr - 0.051; Ni - 0.05; Mo - 0.013; Ti - 0.004; Al - 0.103; Cu - 0.050; Sn - 0.004; B - 0.00105; Co - 0.017; Nb - 0.012; Pb - 0.001 and the remainder is iron. Prior to gravimetric and electrochemical measurements, the surface of the specimens was polished under running tap water using SiC emery paper up to 1200 grade, rinsed with distilled water, dried on a clean tissue paper, immersed in benzene for 5 sec, dried and then immersed in acetone for 5 sec and dried with clean tissue paper. Finally, the specimens were kept in desiccators until use. At the end of the test, the specimens were carefully washed with benzene and acetone, dried and then weighed. Appropriate concentrations of acid were prepared by using double-distilled water. The concentration range of inhibitor employed was 0.3 mM – 1.5 mM.

Synthesis of inhibitors: The synthesis of benzimidazole derivatives is outlined in Scheme 1. To a solution of substituted carboxylic acid (0.01 mol) in THF (10 mL), TBTU (0.01 mol) and DIPEA (Diisopropylethylamine) (0.01 mol) were added and stirred for 20 min at room temperature. 4-Bromo-benzene-1,2-diamine (0.01 mol) was then added and the reaction mixture was refluxed for 4-5 h, After the completion of reaction, reaction mixture was concentrated and extracted with ethyl acetate. The ethyl acetate layer was washed with water, brine, dried over anhydrous sodium sulfate and evaporated under reduced pressure. 6 volumes of acetic anhydrous was added to the concentrated residue and heated up to 45 - 60 ºC for 7-8 h. Then pH was adjusted to neutral using $NaHCO_3$, extracted with ethyl acetate and evaporated to give desired products. The abbreviations, substituents ($R_1$and R_2), molecular structures and names of all the three benzimidazole derivatives are given in table. 1.

All solvents and chemicals used were of analytical reagent grade and used as such. FTIR spectra were recorded using a Jasco FTIR 4100 double beam spectrometer. ^{1}H-NMR spectra were recorded on Bruker DRX-500 spectrometer at 400 MHz using DMSO-d_6 as solvent and TMS as an internal standard. LC - Mass spectra were recorded using Agilent - SC/AD/10-017 instrument.

6-Bromo-2-(3,4-dimethoxy-phenyl)-1H-benzoimidazole (BDB) : IR (KBr) $\square_{max}$ (cm^{-1}): 3430 (N-H), 3038 (Ar-H), 2963 (-CH_3), 2825 (O-CH_3), 1695 (N=C), 1100 (Ar-O), 710 (Ar-Br). ^{1}H-NMR (400.15 MHz, DMSO-d_6) δ ppm: 3.70 (3H, s, OCH_3), 3.76 (3H, s, OCH_3), 6.88 (1H, dd, J = 8.89, J = 2.19, Ar-H), 7.17

(1H, dd, J = 2.49, J = 2.19, Ar-H), 7.29 (1H, s, J = 8.02, J = 1.69, Ar-H), 7.61 (1H, dd, J = 8.89, J = 2.49 benzimidazole-H), 7.67 (1H, dd, J = 8.02, J = 0.48 benzimidazole-H), 7.85 (1H, s, benzimidazole-H). m/z 332.03 (M+), 334.08 (M+2), 333.02 (M+2).

Table 1. The abbreviations, substituent (R_1 and R_2), molecular structures and names of all the benzimidazole derivatives

Abbreviation	R_1	R_2	Molecular structure	Name
BDB	$-OCH_3$	$-OCH_3$	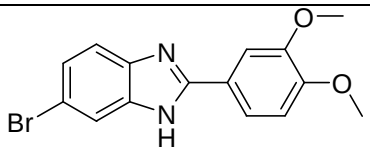	6-Bromo-2-(3,4-dimethoxy-phenyl)-1H-benzoimidazole
BPMP	-H	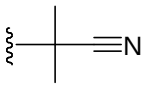	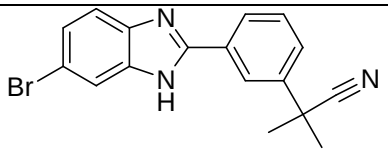	2-[3-(6-Bromo-1H-benzoimidazol-2-yl)-phenyl]-2-methyl-propionitrile
BFB	-F	-H	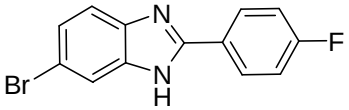	6-Bromo-2-(4-fluoro-phenyl)-1H-benzoimidazole

2-[3-(6-Bromo-1H-benzoimidazol-2-yl)-phenyl]-2-methyl-propionitrile (BPMP) : IR (KBr) $\square_{max}$ (cm^{-1}): 3442 (N-H), 3035 (Ar-H), 2963 ($-CH_3$), 2252 (nitrile group), 1382 and 1368 (C-$(CH_3)_2$), 1691 (N=C), 710 (Ar-Br). ^{1}H-NMR (400 MHz, DMSO-d_6) δ ppm: 1.47 ($2CH_3$, CN $(CH_3)_2$), 7.27 (1H, d, J = 1.70, Ar-H), 7.51 (1H, m, Ar-H), 7.53 (1H, d, J = 7.83, Ar-H), 7.66 (1H, s, Ar-H), 7.82 (1H, dd, J = 8.33, J = 0.69, benzimidazole-H), 7.85 (1H, dd, J = 1.70, J = 0.69, benzimidazole-H), 7.89 (1H, s, benzimidazole-H), m/z 339.8 (M+), 341.4 (M+2), 340.1 (M+1).

6-Bromo-2-(4-fluoro-phenyl)-1H-benzoimidazole (BFB) : IR (KBr) $\square_{max}$: 3448 (N-H), 3032 (Ar-H), 1689 (N = C), 1030 (C-F), 711 (Ar-Br), ^{1}H-NMR (400 MHz, DMSO-d_6) δ ppm: 7.45 (2H, m Ar-H), 7.79 (2H, m, Ar-H), 7.29 (1H, d, J = 8.32, benzimidazole-H), 7.80 (1H, d, J = 8.32, benzimidazole-H), 7.86 (1H, s, benzimidazole-H). m/z 289.9 (M-2), 291.4 (M+1), 290.3 (M+1), 292 (M+2).

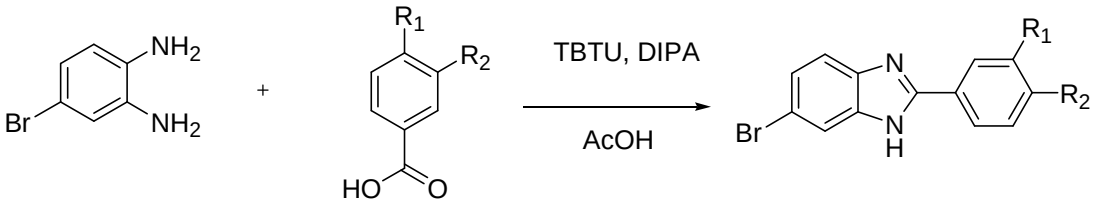

Scheme 1: Scheme for the synthesis of benzimidazole derivatives.

Weight loss measurements: Mild steel specimens were immersed in the acid solutions for 6h at different temperature. The temperature of the environment was maintained by thermostatically controlled water bath with accuracy of ± 0.2 ºC (Weiber limited, Chennai, India), under aerated condition. After 6 h of immersion, the specimens were removed, rinsed in water and acetone, and dried in desiccators. The weight loss was recorded to the nearest 0.0001 g by using analytical balance (Sartorius, precision ± 0.1 mg). The average weight loss of three parallel specimens was obtained. Relative weight loss of the specimens were

used to calculate the percent inhibition efficiency (η %). Then the tests were repeated with different concentrations of the inhibitor at varying temperatures.

Electrochemical measurements: Polarization and Electrochemical Impedance Spectroscopy (EIS) experiments were carried out using a CHI660D electrochemical workstation. A conventional three-electrode cell consisting of a saturated calomel reference electrode (SCE), a platinum auxiliary electrode and the working electrode with 1cm^2 exposed area were used. The specimens were pre-treated similarly as done in the gravimetric measurements. The electrochemical tests were performed using the synthesized benzimidazole derivatives with various concentrations ranging from 0.3 mM – 1.5 mM at 30 ºC. Potentiodynamic polarization measurements were performed in the potential range from -850 to -150 mV with a scan rate of 0.4 mV s^{-1}. EIS measurements were carried out at the open circuit potential (OCP). Prior to EIS measurements, a steady-state period of 30 min was observed which proved sufficient for OCP to attain a stable value. The ac frequency range extended from 10 kHz to 0.05 kHz with signal amplitude of ±10 mV.

Scanning Electron Microscopy (SEM): The SEM analysis was performed using a JSM-5800 electron microscope with the working voltage of 20 kV and the working distance 24 mm. In SEM micrographs, the specimens were exposed to the 0.5 M HCl in the absence and presence of inhibitors under optimum conditions after a desired period of immersion. The SEM images were taken for polished mild steel specimen and specimen immersed in solution with and without inhibitors.

RESULTS AND DISCUSSION

Weight Loss Measurements: The corrosion inhibition efficiencies (%) of the inhibitors BDB, BPMP and BFB after 6 h of immersion at 30 – 60 ºC are evaluated by weight loss method are listed in the Table. 2. From Table 2, it is apparent that the inhibition efficiency increased with increasing concentration (0.3 mM – 1.5 mM) of each inhibitor. This observation can be attributed to an increase in the number of inhibitor molecules adsorbed on the metal surface, which separate the mild steel from the acid solution, resulting in the retardation of metal dissolution [29]. The inhibition efficiency of the inhibitors followed the order BDB >BPMP> BFB (Fig. 1). The corrosion rate (C_R) was calculated from the following equation:

$$C_R = \frac{\Delta W}{St} \qquad (1)$$

where, ΔW is the weight loss (mg cm^{-2} h^{-1}), S is the surface area of the specimen (cm^2) and t is the immersion time (h). The corrosion inhibition efficiency (%) was calculated according to the equation (2)

$$\eta(\%) = \frac{(C_R)_a - (C_R)_p}{(C_R)_a} \times 100 \qquad (2)$$

where $(C_R)_a$ and $(C_R)_p$ are corrosion rates in the absence and presence of the inhibitor, respectively. The corrosion parameters namely, the corrosion rate (CR), surface coverage (θ) and inhibition efficiency (%) of mild steel in 0.5 M HCl in the presence and absence of inhibitors at different temperatures obtained from weight loss measurements are listed in table 2. The inhibitor was found to attain the maximum inhibition efficiency at 1.5 mM for all the studied inhibitors (fig. 1). This is due to the fact that, adsorption and the degree of surface coverage of inhibitor on the mild steel increases with the inhibitor concentration, thus the mild steel surface gets efficiently separated from the medium [30]. The protective property of these compounds is probably due to the interaction between p electrons and hetero atoms with positively charged steel surface [31]. In the absence of any inhibitor, the corrosion rate of mild steel increased steeply with the increase in temperature (30 – 60 ºC), whereas in the presence of inhibitors, the corrosion rate decreases for all three studied inhibitors. The corrosion rate was much lower in the presence of inhibitor than in its absence at each temperature (fig. 1).

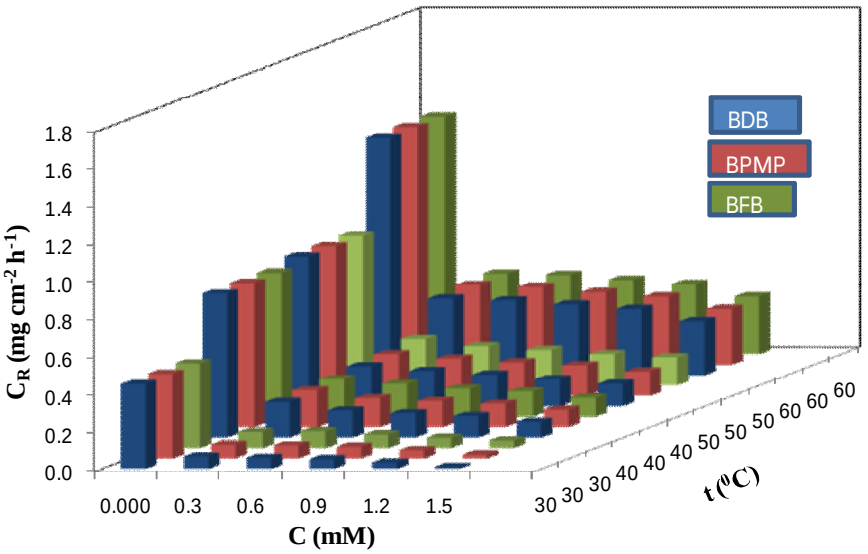

Figure 1 Variation of CR as a function of temperature and concentration of BDB, BPMP and BFB.

Table 2. Weight loss data of mild steel corrosion in 0.5 M HCl in presence of different concentrations of the inhibitors at different temperature

Inhibitor	C (mM)	30 °C C_R in (mg cm^{-2} h^{-1})	□	□ (%)	40 °C C_R in (mg cm^{-2} h^{-1})	□	□ (%)	50 °C C_R in (mg cm^{-2} h^{-1})	□	□ (%)	60 °C C_R in (mg cm^{-2} h^{-1})	□	□ (%)
Blank	-	0.452	-	-	0.765	-	-	0.796	-	-	1.260	-	-
BDB	0.3	0.067	0.852	85.2	0.191	0.750	75.0	0.215	0.730	73.0	0.406	0.678	67.8
	0.6	0.061	0.865	86.5	0.146	0.809	80.9	0.191	0.760	76.0	0.396	0.686	68.6
	0.9	0.053	0.883	88.3	0.131	0.829	82.9	0.171	0.785	78.5	0.374	0.703	70.3
	1.2	0.035	0.923	92.3	0.116	0.848	84.8	0.146	0.817	81.7	0.351	0.721	72.1
	1.5	0.011	0.976	97.6	0.084	0.890	89.0	0.122	0.847	84.7	0.285	0.774	77.4
BPMP	0.3	0.074	0.836	83.6	0.198	0.741	74.1	0.224	0.719	71.9	0.423	0.664	66.4
	0.6	0.071	0.843	84.3	0.156	0.796	79.6	0.201	0.747	74.7	0.412	0.673	67.3
	0.9	0.063	0.861	86.1	0.141	0.816	81.6	0.181	0.773	77.3	0.384	0.695	69.5
	1.2	0.045	0.900	90.0	0.126	0.835	83.5	0.165	0.793	79.3	0.361	0.713	71.3
	1.5	0.021	0.954	95.3	0.094	0.877	87.7	0.132	0.834	83.4	0.295	0.766	76.6
BFB	0.3	0.087	0.808	80.8	0.202	0.736	73.6	0.249	0.687	68.7	0.429	0.659	65.95
	0.6	0.091	0.799	79.9	0.176	0.770	77.0	0.211	0.735	73.5	0.422	0.665	66.50
	0.9	0.073	0.839	83.8	0.151	0.803	80.3	0.191	0.760	76.0	0.394	0.687	68.73
	1.2	0.055	0.878	87.8	0.136	0.822	82.2	0.169	0.788	78.8	0.371	0.706	70.55
	1.5	0.041	0.909	90.9	0.103	0.865	86.5	0.152	0.809	80.9	0.305	0.758	75.79

Thermodynamic and activation parameters: Thermodynamic and activation parameters play important role in understanding the inhibition mechanism. The weight loss measurements were performed in the temperature range of 30 – 60 ºC in the absence and presence of different concentrations of inhibitors (0.3 mM – 1.5 mM) during 6h of immersion time in 0.5 M HCl for mild steel. The C_R gets increased with the rise in temperature in the uninhibited solution, but in the presence of inhibitor, C_R gets highly reduced (Fig. 1). Hence, inhibition efficiency decreases with the rise in temperature. It may be due to the fact that, higher temperature accelerates hot-movement of the organic molecules and weakens the adsorption capacity of inhibitor on the metal surface [32, 33].

The activation energy (E_a^*) for dissolution of MS can be expressed using the Arrhenius equation.

$$C_R = k\, exp\left(-\frac{E_a^*}{RT}\right) \quad (3)$$

An alternative formulation of the Arrhenius equation is,

$$C_R = \frac{RT}{Nh} exp\frac{\Delta S_a^*}{R} exp\left(-\frac{\Delta H_a^*}{RT}\right) \quad (4)$$

where, k is Arrhenius pre-exponential factor, h is Planck's constant, N is Avogadro's number, T is the absolute temperature and R is the universal gas constant. Using Eq. (3), and from a plot of the ln C_R *versus* 1/T (Fig. 2a - 2c), the values of E_a^* and k at various concentrations of BDB, BPMP and BFB were computed from slopes and intercepts, respectively (Table 3). Further, using Eq. (4), plots of ln (C_R/T) *versus* 1/T gave straight lines (Fig 3a - 3c) with a slope of (-ΔH_a^*/2.303R) and an intercept of [log (R/Nh) + ΔS_a^*/2.303R], from which the values of ΔH_a^* and ΔS_a^* were calculated and are listed in Table 3. Generally, the values of the activation energy for the inhibited solutions are lower than that of the uninhibited solution, indicating a chemisorption process of adsorption [34], whereas higher values of E_a^* indicates a physical adsorption mechanism [35]. In the present study, the values of E_a^* in inhibited solution are increases when compared to uninhibited acid solutions (Table 3). This supports physisorption of BDB, BPMP, and BFB on mild steel surface.

The positive sign of the activation enthalpy (ΔH_a^*) reflects the endothermic nature of the mild steel dissolution process [36, 37]. The negative value of ΔS_a^* for all three inhibitors indicates that the formation of the activated complex in the rate- determining step represents an association rather than a dissociation step, meaning that a decrease in disorder takes place during the course of the transition from reactants to activated complex [38].

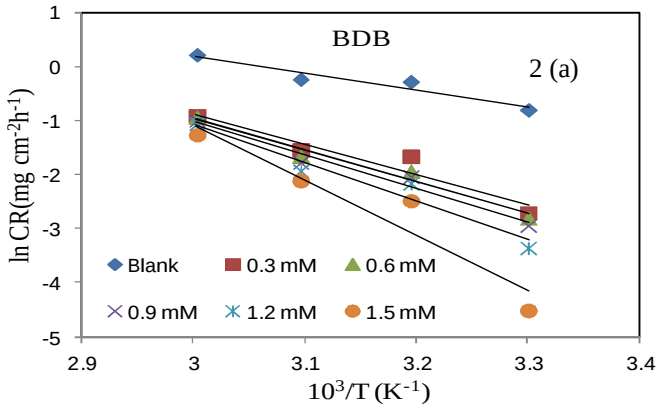

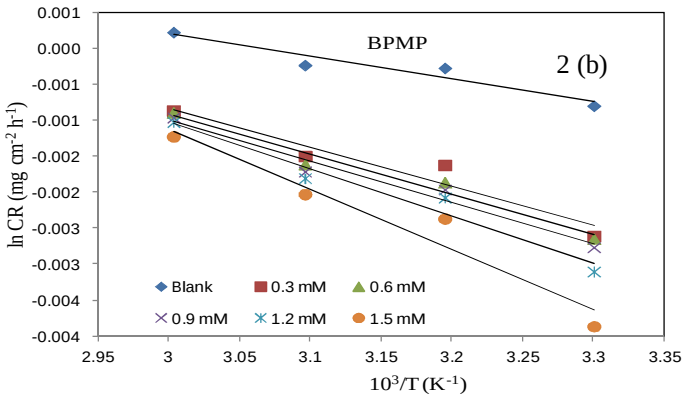

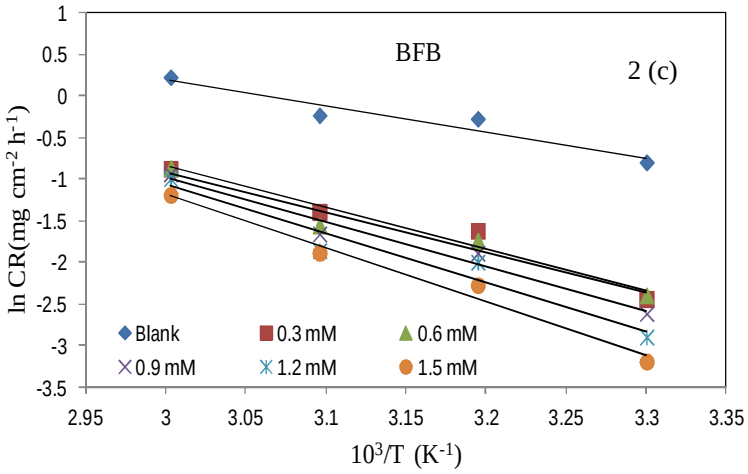

Figure 2 Arrhenius plots for the corrosion of mild steel in 0.5 M HCl in the absence and presence of different concentrations of (a) BDB, (b) BPMP and (c) BFB.

Table 3. Activation parameters for mild steel in 0.5 M HCl in the absence and presence of different concentrations of BDB, BPMP, and BFB

Inhibitor	C (mM)	E^*_a kJ/mol^{-1}	k mg cm^{-2} h^{-1}	ΔH_a^* kJ mol^{-1}	$\Delta H_a^* = E_a^* - RT$ kJ mol^{-1}	ΔS^* J mol^{-1} K^{-1}
BDB	0	26.15	15336	23.50	23.38	-173.62
	0.3	46.49	8040485	43.85	43.72	-121.49
	0.6	49.38	21210353	46.73	46.60	-113.49
	0.9	51.45	41866644	48.80	48.68	-107.83
	1.2	60.09	910951303	57.45	57.32	-82.22
	1.5	85.62	9015802617883	82.98	82.85	-5.74
BPMP	0	26.15	15336	24.50	23.38	-170.25
	0.3	45.07	4975318	42.43	42.30	-125.52
	0.6	46.38	7422303	43.75	43.61	-122.22
	0.9	47.58	10532749	44.94	44.81	-119.28
	1.2	54.76	137619061	52.30	52.00	-97.94
	1.5	69.68	27024237893	67.04	66.91	-54.04
BFB	0	26.15	15336	23.50	23.38	-173.62
	0.3	36.72	237993	34.087	34.087	-150.75
	0.6	39.66	640497	37.022	37.022	-142.60
	0.9	43.90	2757955	41.254	41.254	-130.39
	1.2	49.78	21638831	47.149	47.149	-113.32
	1.5	53.85	85156389	51.214	51.214	-101.93

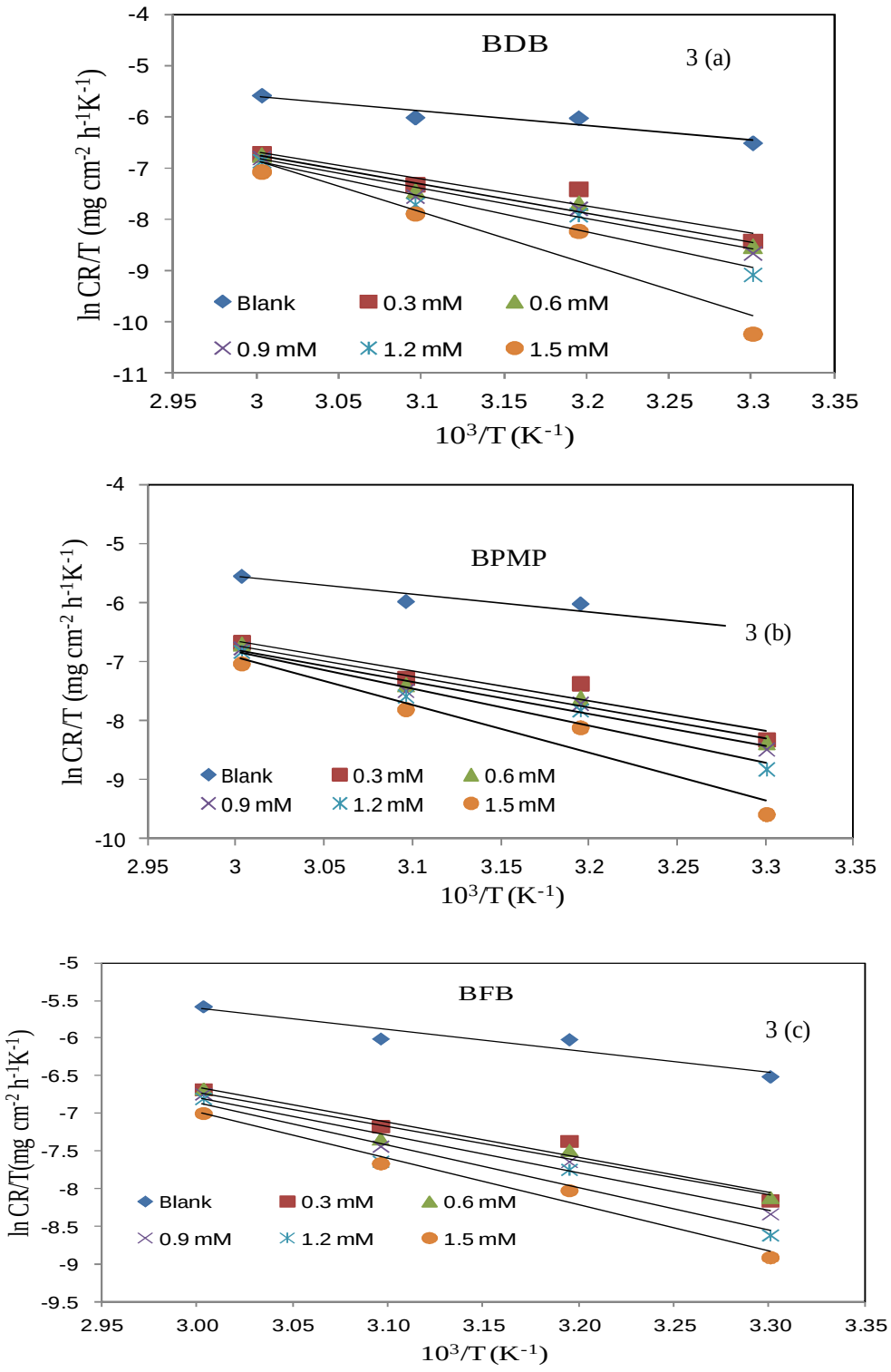

Figure 3 Alternative Arrhenius plots for mild steel in 0.5 M HCl in the absence and presence of different concentrations of (a) BDB, (b) BPMP and (c) BFB.

Adsorption isotherm: The basic information on the interaction between an organic inhibitor and a mild steel surface can be obtained from various adsorption isotherms. The most commonly used adsorption isotherms are the Langmuir, Temkin and Frumkin isotherms. The surface coverage (θ) for different concentrations of inhibitor in 0.5 M hydrochloric acid was tested graphically to determine a suitable adsorption isotherm. Plots of C/θ versus C yielded straight lines (Fig 4a - 4c) with correlation co-efficient (R^2) values close to unity. This indicates that the adsorption of these inhibitors can be fitted to the Langmuir adsorption isotherm. According to Langmuir adsorption isotherm there is no interaction between the adsorbed inhibitor molecules, and the energy of adsorption is independent on the degree of surface coverage (θ). Langmuir isotherm assumes that the solid surface contains a fixed number of adsorption sites and each site occupies one adsorbed species. According to this isotherm, θ is related to the inhibitor concentration, C and adsorption equilibrium constant K_{ads}, as

$$\frac{C}{\theta} = \frac{1}{K_{\text{ads}}} + C \qquad (5)$$

From the intercepts in Fig. 4, values of K_{ads} were calculated. The large values of K_{ads} obtained for all three studied inhibitors imply efficient adsorption, and hence, good corrosion inhibition efficiency. Using the calculated values of K_{ads}, ΔG_{ads} was evaluated according to the equation,

$$K_{\text{ads}} = \frac{1}{55.5} exp\left[\frac{\Delta G_{ads}}{RT}\right] \qquad (6)$$

where R is the gas constant and T is the absolute temperature (K). The value of 55.5 is the concentration of water in solution (mol L^{-1}). Using the plot of ΔG_{ads} *vs* T (Fig. 5) the value of ΔS_{ads} and ΔH_{ads} were computed from slope and intercept, respectively. The calculated ΔG_{ads}, ΔS_{ads} and ΔH_{ads} values of the studied benzimidazole derivatives are tabulated in table 4.

It is generally accepted that, the values of ΔG_{ads} up to -20 kJ/mol, the adsorption can be regarded as physisorption, in which case inhibition results from the electrostatic interactions between the charged molecules of the inhibitors and the charged metallic surface. In contrast, for values above -40 kJ/mol, the adsorption is regarded as chemisorption, which is due to charge sharing or transfer from the inhibitor molecules to the metal surface to form a covalent bond [39]. The values of ΔS_{ads} and ΔH_{ads} give information about the mechanism of corrosion. The negative value of ΔH_{ads} indicates that adsorption process is exothermic. An exothermic adsorption process may be chemisorption or physisorption or mixture of both [40] whereas endothermic process is attributed to chemisorption [41]. In exothermic adsorption process, physisorption can be distinguished from the chemisorption on the basis of ΔH_{ads} values. For physisorption process, the magnitude of ΔH_{ads} is around - 40 kJ mol^{-1} or less negative while its value - 100 kJ mol^{-1} or more negative for chemisorptions [42].

In the present work, the calculated ΔG_{ads} values (table 4) between -15.79 to -17.36 indicated that the adsorption mechanism of the synthesized benzimidazole derivatives on mild steel in 0.5 M HCl solution is physisorption. The negative value of ΔH_{ads}, again confirmed that benzimidazole derivatives adsorb on the mild steel surface through physisorption. The value of ΔS_{ads} is negative for all the inhibitor implies that the activated complex in the rate determining step represents an association rather than a dissociation step, meaning that a decrease in disordering takes place on going from reactants to the activated complex [43].

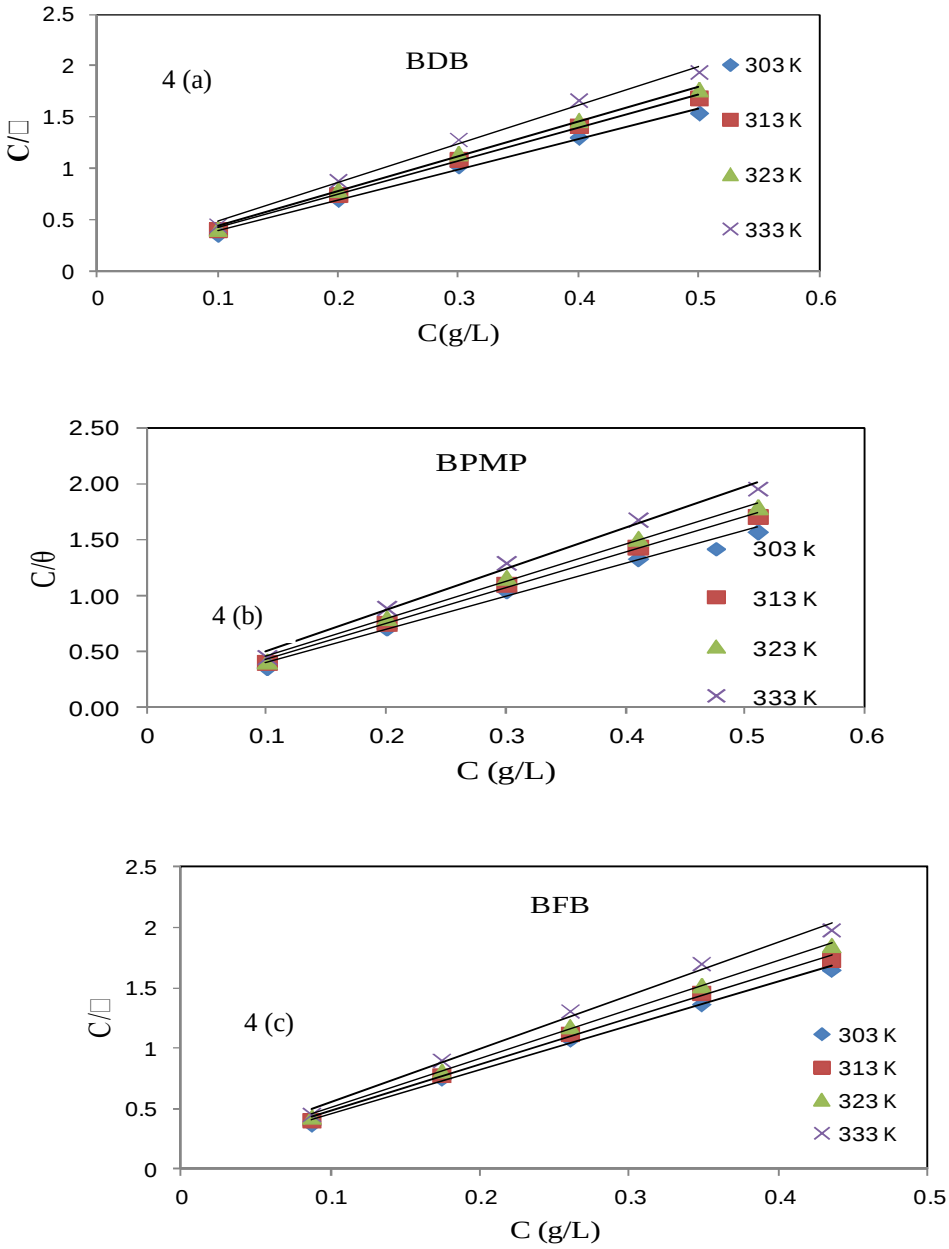

Figure 4 Langmuir isotherm for the adsorption of (a) BDB (b) BPMP and (c) BFB on mild steel in 0.5 M HCl at different temperatures.

Table 4. Thermodynamic parameters for adsorption of BDB, BPMP and BFB on mild steel in 0.5 M HCl at different temperatures from Langmuir adsorption isotherm

Inhibitor	T (K)	R^2	K_{ads} (L mol^{-1})	ΔG_{ads} (kJ mol^{-1})	ΔH_{ads} (kJ mol^{-1})	ΔS_{ads} J mol^{-1}K^{-1}
BDB	303	0.994	11494.25	-16.27	-5.194	-36
	313	0.997	10869.57	-16.66		

	323	0.997	10309.28	-17.05		
	333	0.993	9523.81	-17.36		
BPMP	303	0.992	9523.81	-15.79	-6.380	-31
	313	0.997	9090.91	-16.20		
	323	0.996	8695.65	-16.59		
	333	0.992	7518.80	-16.70		
BFB	303	0.996	10989.01	-16.16	-6.132	-33
	313	0.997	9900.99	-16.42		
	323	0.998	9900.99	-16.94		
	333	0.993	8620.69	-17.08		

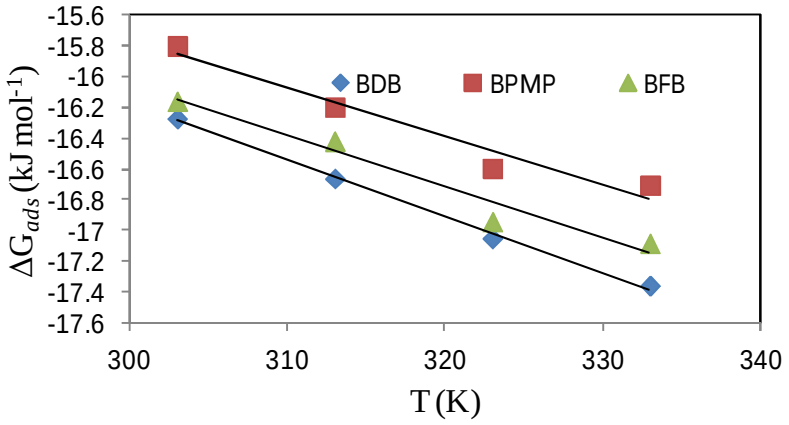

Figure 5 Plot of ΔG_{ads} *vs*. absolute temperature of (a) BDB (b) BPMP and (c) BFB.

Potentiodynamic polarization: The potentiodynamic polarization curves obtained from the corrosion behavior of mild steel in 0.5 M HCl in the absence and presence of BDB, BPMP and BFB are shown in Fig. 6a-6c. The electrochemical parameters such as corrosion potential (E_{corr}), corrosion current density (I_{corr}), Tafel slopes [(i.e. cathodic (β_c) and anodic (β_a)] obtained from the polarization measurements are listed in Table 5. The η% was calculated using the following equation:

$$\eta\% = \frac{(I_{corr})_a - (I_{corr})_p}{(I_{corr})_a} \times 100 \qquad (7)$$

where, $(I_{corr})_a$ and $(I_{corr})_p$ are the corrosion current density (mA cm^{-2}) in the absence and presence of the inhibitor, respectively. From the potentiodynamic polarization curves, it can be clearly seen that I_{corr} decreases and η% increases with increasing inhibitor concentration. The cathodic and anodic Tafel slope values changed with the inhibitor concentration, indicating that benzimidazole derivatives controlled both the cathodic hydrogen evolution and anodic mild steel dissolution reactions [44]. The corrosion potential E_{corr} values do not show any appreciable shift i.e., not more than 85 mV with respect to the corrosion potential of blank solution, which suggest that all the three inhibitors acted as mixed type [45]. From the Tafel slopes it was evident that anodic reaction is more polarized when an external current density is applied ($\beta_a > \beta_c$), which indicates more pronounced anodic inhibition. Among the synthesized

benzimidazole derivatives, BDB shows highest inhibition efficiency. The order of inhibition efficiency was BDB > BPMP > BFB.

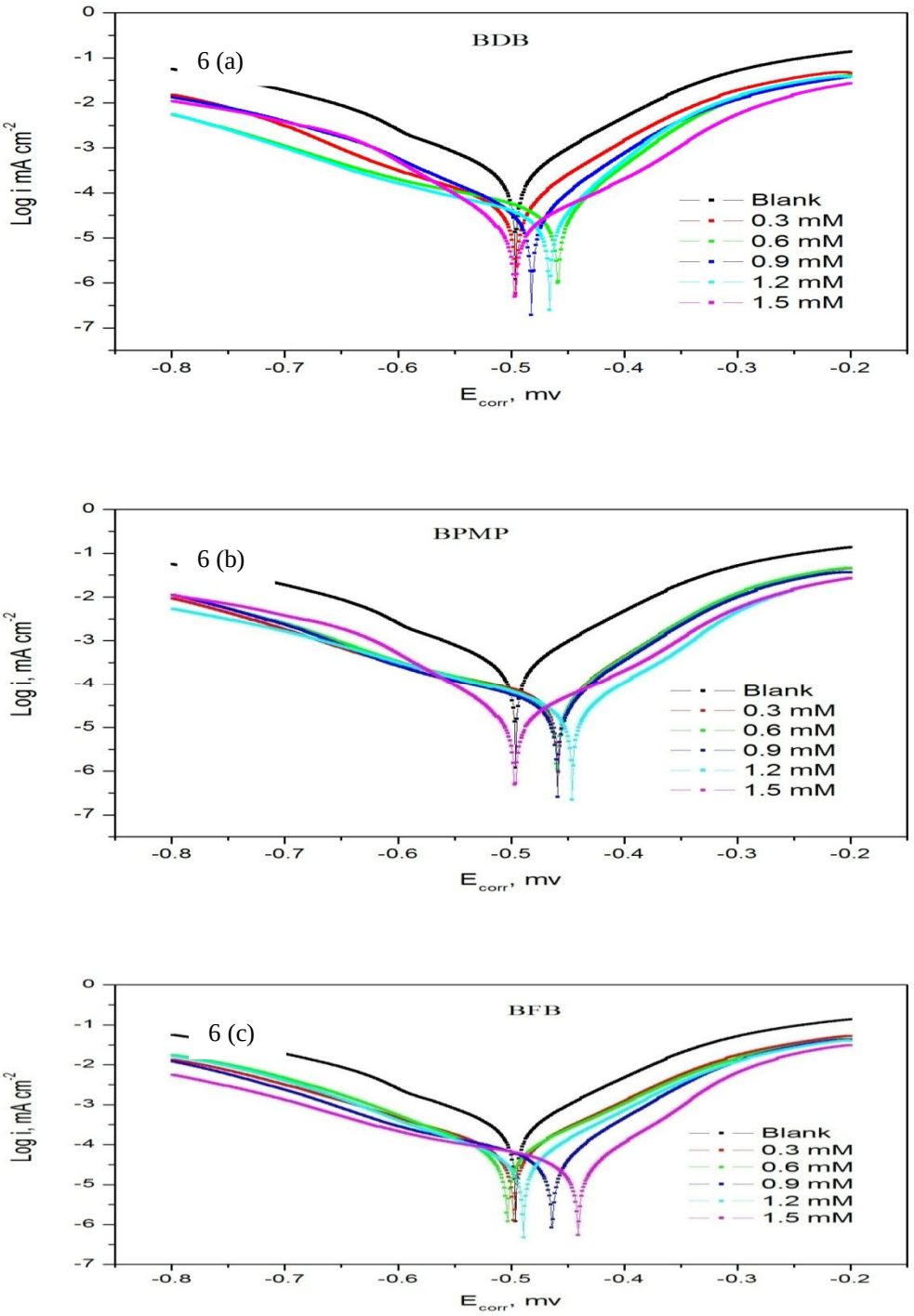

Figure 6 Polarization curves for mild steel in 0.5 M HCl containing different concentration of (a) BDB (b) BPMP and (c) BFB.

Electrochemical impedance spectroscopy: Nyquist plots of mild steel in 0.5 M HCl solution in the absence and presence of different concentrations of BDB, BPMP and BFB at 30 ºC are shown in Fig (7a-7c). Nyquist impedance plots were analyzed by fitting the experimental data to a simple circuit model (Fig. 8) that includes the solution resistance (R_s), charge transfer resistance (R_{ct}) and double layer capacitance (C_{dl}). The values are presented in Table. 6. The η% was calculated using the charge transfer using equation (8).

$$\eta\% = \frac{{}^{1}/_{(R_{ct})_a} - {}^{1}/_{(R_{ct})_p}}{{}^{1}/_{(R_{ct})_a}} \times 100 \qquad (8)$$

Table 5. Potentiodynamic polarization parameters for the corrosion of mild steel in 0.5 M HCl in absence and presence of different concentrations of BDB, BPMP and BFB inhibitors at 30º C

Inhibitor	*C(mM)*	E_{corr} *(mV (SCE))*	I_{corr} (mA cm^{-2})	β_a mV dec^{-1}	β_c mV dec^{-1}	□ (%)
Blank	-	-496	0.2730	13.155	9.909	-
BDB	0.3	-496	0.0542	15.411	7.879	80.12
	0.6	-459	0.0408	17.62	4.891	85.04
	0.9	-482	0.0340	15.87	10.063	87.51
	1.2	-466	0.0297	19.381	5.715	89.11
	1.5	-497	0.0174	12.757	14.493	93.60
BPMP	0.3	-458	0.0555	16.448	5.572	79.66
	0.6	-459	0.0468	6.397	17.168	82.85
	0.9	-459	0.0399	6.057	17.002	85.39
	1.2	-437	0.0326	14.819	6.399	88.05
	1.5	-470	0.0169	19.507	12.107	93.81
BFB	0.3	-498	0.0750	13.048	8.381	72.50
	0.6	-503	0.0597	13.061	10.843	78.13
	0.9	-464	0.0470	5.571	15.782	82.74
	1.2	-489	0.0432	14.383	9.677	84.17
	1.5	-441	0.0357	16.103	4.381	86.90

The impedance spectra (fig. 7) exhibit semicircle which can be attributed to the charge transfer that takes place at electrode/solution interface and this process controls the corrosion of mild steel. On the other hand, some Nyquist plots are not perfect semicircle, which is attributed to surface inhomogeneity and roughness [46]. It is evident from these plots that the impedance response of mild steel in uninhibited acid solution has significantly changed after the addition of the inhibitor in the aggressive solution. It is apparent from Table 6 that the value of R_{ct} increased with increasing concentration of inhibitors. The increase in R_{ct} values is attributed to the formation of an insulating protective film at the metal/solution interface. It is also clear that the value of C_{dl} changed upon the addition of each of the inhibitors, indicating a decrease in the local dielectric constant and/or an increase in the thickness of the electrical double layer, suggesting that the inhibitors function by forming a protective layer at the metal surface [47]. Therefore, the changes in R_{ct} and C_{dl} were caused by the steady replacement of water molecules by the adsorption of inhibitor on the mild steel surface, reducing the extent of metal dissolution [48]. The results obtained by potentiodynamic polarization, electrochemical impedance spectroscopy (EIS) and weight loss measurements are in reasonable agreement with each other.

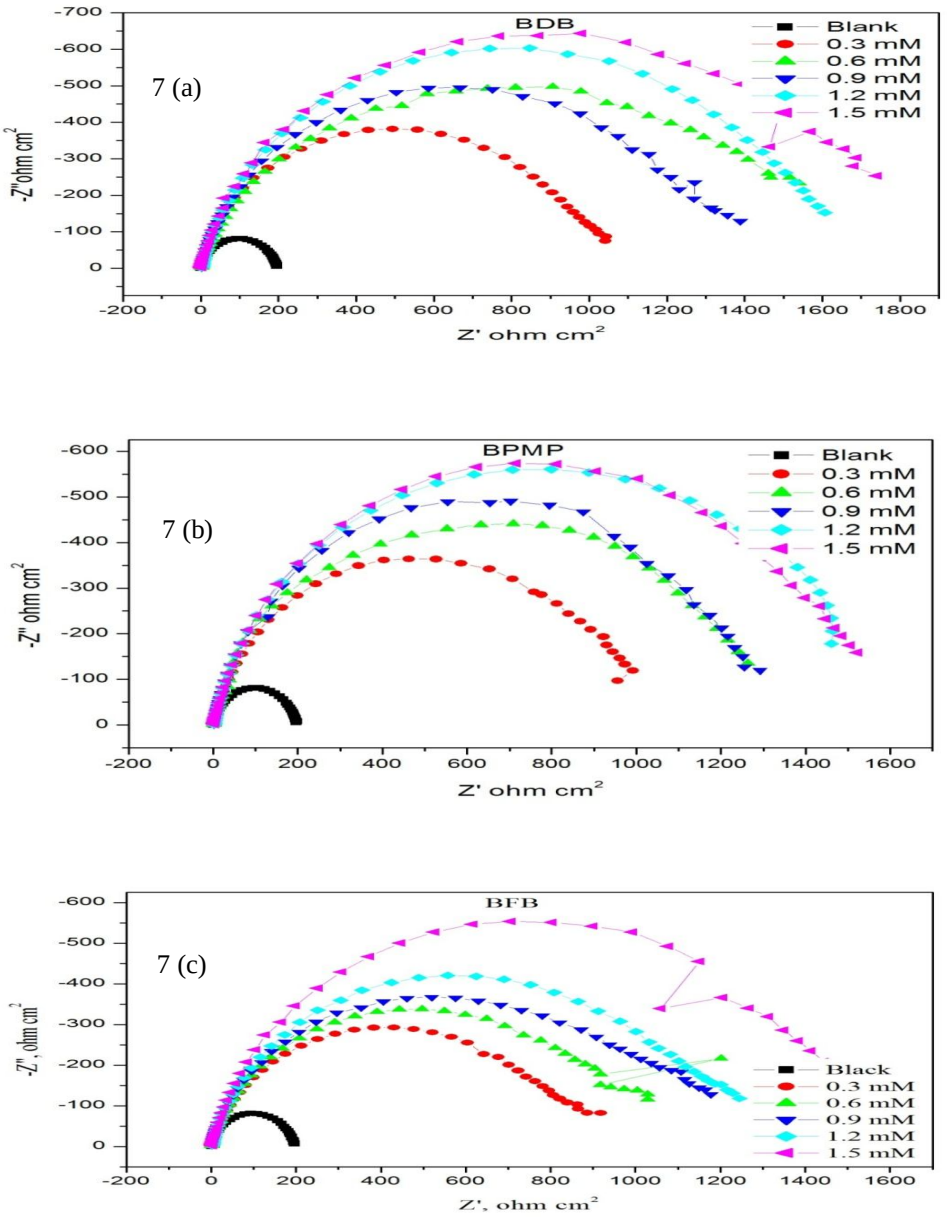

Figure 7 Nyquist plots in the absence and presence of different concentrations of of (a) BDB, (b) BPMP and (c) BFB in 0.5 M HCl.

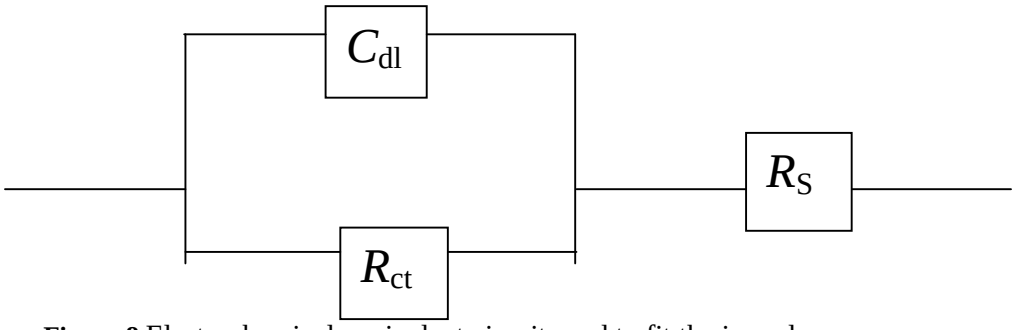

Figure 8 Electrochemical equivalent circuit used to fit the impedance.

Table 6. Impedance parameters for the corrosion of mild steel in 0.5 M HCl in presence of different concentration of the BDB, BPMP and BFB

Inhibitor	C (mM)	R_{ct} (Ω cm^2)	C_{dl} (μF cm^{-2})	□ (%)
Blank	-	170.4	162	-
BDB	0.3	851.6	233	79.99
	0.6	1025.0	201	83.37
	0.9	1079.0	240	84.21
	1.2	1295.0	226	86.84
	1.5	1353.0	261	87.40
BPMP	0.3	807.5	379	78.90
	0.6	940.1	360	81.87
	0.9	1058.0	332	83.89
	1.2	1209.0	287	85.90
	1.5	1231.0	232	86.16
BFB	0.3	664.7	235	74.36
	0.6	765.4	199	77.74
	0.9	859.2	135	80.17
	1.2	959.3	134	82.24
	1.5	1192.0	233	85.70

Morphological Investigation: The SEM micrographs obtained for the mild steel surface in the absence and presence of optimum concentration (1.5 mM) of the inhibitors in 0.5 M HCl at 6 h immersion time and 30 ºC are shown in Fig. 9a-9e. The image of the polished mild steel is shown in Fig. 9 a. The mild steel surface in the absence of inhibitors exhibited a highly corroded surface with pits and cracks (Fig. 9 b). This is due to the attack of mild steel surface with aggressive acid medium. However, in the presence of BDB (Fig. 9 c) BPMP (Fig. 9 d) and BFB (Fig. 9 e) the mild steel surface could be observed with a thin layer of the inhibitor molecules, giving protection against corrosion. The inhibited mild steel surface was smoother than the uninhibited surface indicating the presence of a protective layer of adsorbed inhibitors preventing acid attack. The formed surface film has higher stability and low permeability in aggressive solution than uninhibited mild steel surface. Hence, they show an enhanced surface properties which seemed to provide corrosion protection to the mild steel beneath them by restricting the mass transfer of reactants and products between the bulk solution and the mild steel surface.

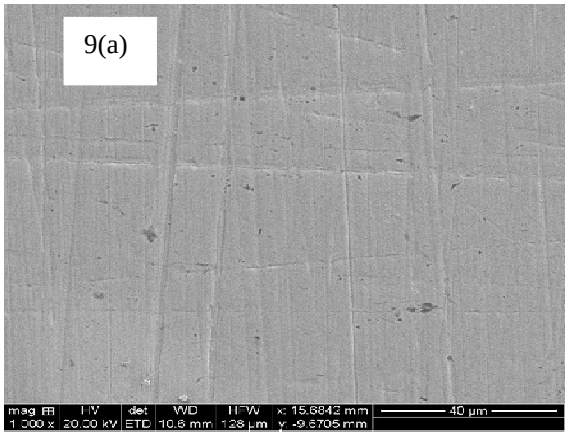

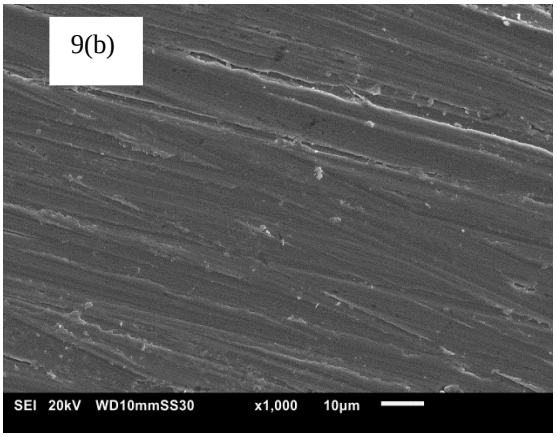

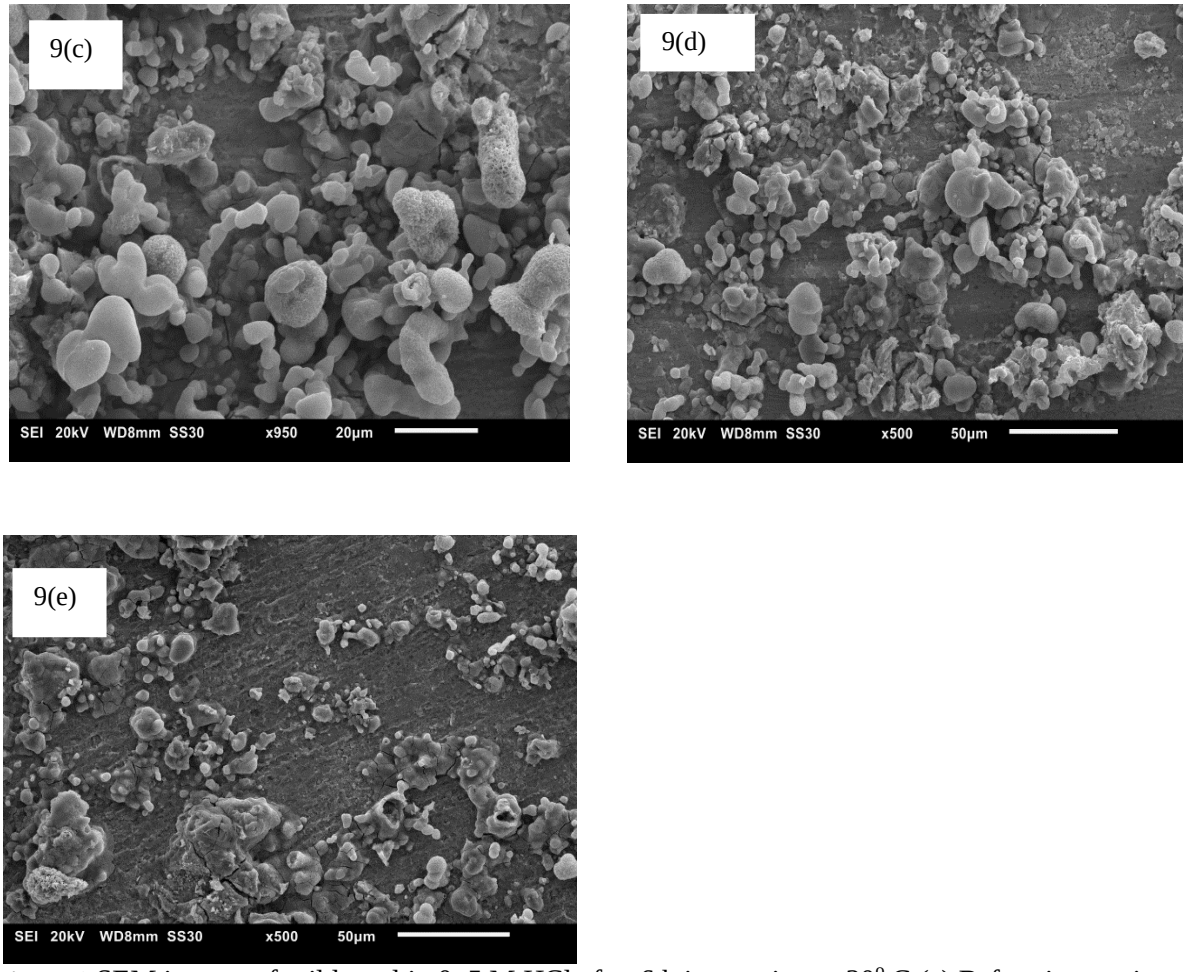

Figure 9 SEM images of mild steel in 0. 5 M HCl after 6 h immersion at 30^{o} C (a) Before immersion (polished) (b) without inhibitor (c) with 1.5 mM of BDB (d) with 1.5 mM of BPMP (e) with 1.5 mM of BFB in 0.5 M HCl.

Inhibition mechanism: As far as the inhibition process is concerned, it is generally assumed that adsorption of an organic inhibitor at the metal/solution interface is the first step in the mechanism of inhibition in aggressive media. Four types of adsorption may take place during inhibition involving organic molecules at the metal/solution interface. (a) Electrostatic attraction between charged molecules and the charged metal (b) interaction of unshared electron pairs in the molecule with the metal (c) interaction of p-electrons with the metal and (d) a combination of the above situations [49]. Further, corrosion inhibition efficiency depends on several factors such as the number of adsorption sites and their charge density, molecular size, heat of hydrogenation, mode of interaction with the metal surface and the formation metallic complexes [50]. Based on the experimental results obtained, we could propose a probable mechanism for corrosion inhibition of benzimidazole derivatives in 0.5 M HCl. The polarization data suggested the mixed inhibition mechanism of benzimidazole derivatives. In acid media, benzimidazole derivatives might be protonated as follows:

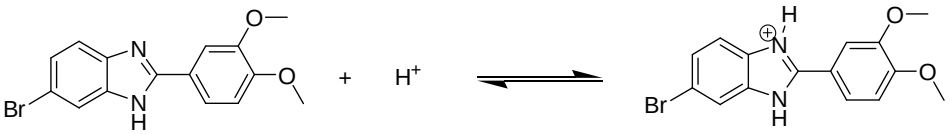

(9)

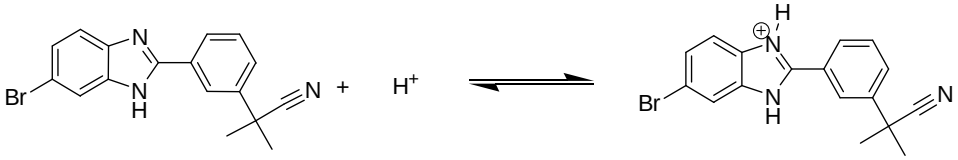

(10)

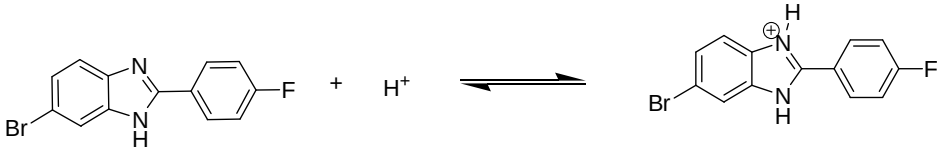

(11)

The cationic forms of inhibitor molecules may be adsorbed directly at the cathodic sites and hinder the hydrogen evolution reaction. In acid solutions, mild steel possesses positive charge at the corrosion potential. The chloride ions present in the solution get adsorbed on metal surface by creating an excess negative charge towards solution and it favours the adsorption of protonated inhibitor molecules on metal surface through electrostatic attraction [51, 52]. Therefore the protonated inhibitor molecules get adsorbed on mild steel surface by means of electrostatic interaction between chloride ions and inhibitor cations (physisorption). In acidic solution, the nitrogen atoms of the benzimidazole molecules can absorb on the cathodic sites of mild steel in competition with the hydrogen ions. The adsorption of benzimidazole molecules on the mild steel surface can be attributed to adsorption of the organic compounds via nitrogen atoms and benzene ring in all cases. The adsorption will take place through the delocalized p-electrons of the benzene ring and also through electron releasing group ($–OCH_3$).

Among the compounds investigated in this study, BDB had the best performance. This could be due to two methoxy ($–OCH_3$) groups, which is an electron donator, strongly activated due to the presence of lone pair of electrons on the oxygen (O) atom, therefore, electron density on the benzene ring increases. However, dimethyl-propionitrile [$(–C(CH_3)_2CN)$] and fluorine (–F) groups are weaker electron donors (moderately activating) than methoxy ($–OCH_3$) groups and hence compounds BPMP and BFB showed lower inhibition efficiencies than BDB.

APPLICATIONS

This study is useful to investigate the inhibition of benzimidazole derivatives on the corrosion of mild steel in 0.5 mM using weight loss, potentiodynamic polarization and electrochemical impedance spectroscopy techniques. The synthesised benzimidazole derivatives are of industrial importance, which may solve the problem of corrosion in heat treatment plant and chillier unit.

CONCLUSIONS

1. All the studied benzimidazole derivatives shown excellent inhibition property for the corrosion of mild steel in 0.5 M HCl solutions, and the inhibition efficiency increases with increasing concentration of the inhibitors.
2. The inhibition ability of these compounds follow the order BDB > BPMP > BFB, and the inhibition efficiencies determined by polarization, EIS and weight loss methods are in reasonable agreement with each other.

3. The adsorption of all the studied molecules obeys the Langmuir isotherm model. The negative values of free energy of adsorption indicated that the adsorption of the benzimidazole molecule is spontaneous process.
4. The results obtained from potentiodynamic polarization indicated that the synthesized inhibitors represent a mixed-type of inhibitors.
5. The calculated ΔG_{ads} and ΔH_{ads} values indicated that the adsorption mechanism of the synthesized benzimidazole derivatives on mild steel in 0.5 M HCl solution is physisorption.
6. SEM analysis shows that the formed surface film has higher stability and low permeability in aggressive solution than uninhibited mild steel surface. Hence, they show enhanced surface properties.

ACKNOWLEDGEMENTS

Authors would like to thank Dr. Arthob Naik and Basavanna Shivarudhraiah, Department of Chemistry, Kuvempu University, Shankaraghatta, Shimoga, India for their help to carryout electrochemical work.

REFERENCES

[1] T. Shahrabi, H. Tavakholi, M. G. Hosseini, *Anti. Corros. Method M.* **2007**, 54, 308 - 313.
[2] H. Xiangqi, L. Chenghao, H. Naibao, *J. Iron Steel Res. Int.* **2006**, 13, 56-60.
[3] M. Dahmani, A. Et-Touhami, S. S. Al-Deyab, B. Hammouti, A. Bouyanzer, *Int. J. Electrochem. Sci.* **2010,** 5, 1060-1069.
[4] J. M. Bastidas, J. L. Polo, E. Cano, *J. Electrochem. Soc.* **2000,** 30, 1173-1177.
[5] M. A. Amin, S. S. Abd El-Rehim, E. E. F. El-Sherbini, R. S. Bayoumi, *Electrochim. Acta* **2007**, 52, 3588-3600.
[6] W. D. Collins, R. E. Weyers, I. L. Al-Qadi, *Corrosion.* **1993,** 49, 74-78.
[7] S. Tamilselvi, V. Raman, N. Rajendran, *J. Appl. Electrochem.* **2003**, 33, 1175-1182.
[8] M. M. Antonijevic, G. D. Bogdanovic, M. B. Radovanovic, M. B. Petrovic, A. T. Stamenkovic, *Int. J. Electrochem. Sci.* **2009**, 4, 654-661.
[9] F. Bentiss, M. Lebrini, H. Vezin, M. Lagrenee, *Mater. Chem. Phys.* **2004**, 87, 18-23.
[10] L. Herrag, A. Chetouani, S. Elkadiri, B. Hammouti, A. Aouniti, *Port. Electrochim. Acta* **2008,** 26, 211-220.
[11] A. E. Ouafi, B. Hammouti, H. Oudda, S. Kertit, R. Touzani, A. Ramdani, *Anti. Corros. Method M.* **2002**, 49 199-204.
[12] M. A. Quraishi, R. Sardar, *Corrosion* **2002**, 58, 748-755.
[13] L. Wang, M. J. Zhu, F. C. Yang, C. W. Gao, *Int. J. Corros.* **2012,** doi: 10.1155/2012/573964
[14] P. Liu1, X. Fang, Y. Tang, C. Sun, C. Yao, *Mater. Sci. Appl.* **2011**, 2, 1268-1278.
[15] F. Chaouket B. Hammouti, S. Kertit, K. E. Kacemi, *Bull. Electrochem.* **2001**, 17, 311-320.
[16] G. K. Gomma, M. H. Wahdan, *Mater. Chem. Phys.* **1997,** 47, 176-183.
[17] K. Tebbji, A. Aouniti, A. Attayibat et al., *Indian J. Chem. Technol.* **2011,** 18, 244–253.
[18] X. M. Wang, H. Y. Yang, F. H. Wang, *Corros. Sci.* **2010**, 52, 1268-1276.
[19] X. M. Wang, H. Y. Yang, F. H. Wang, *Corros. Sci.* **2011,** 53, 113-121.
[20] I. B. Obot, N. O. Obi-Egbedi, S. Z. Umoren, *Corros. Sci*., **2009,** 51, 276-282.
[21] L. Herrag, B. Hammouti, S. Elkadiri, A. Aouniti, C. Jama, H. Vezin, F. Bentiss, *Corros. Sci*. **2010,** 52, 3042-3051.
[22] X. H. Li, S. D. Deng, H. Fu, *Corros. Sci*., **2011**, 53, 302-309.
[23] S. L. Granese, B. M. Rosales, C. Oviedo, J. O. Zerbino, *Corros. Sci*., **1992**, 33, 1439-1453.
[24] J. Cruz, R. Martinez, J. Genesca, E. Garcia-Ochoa, *J. Electroana. Chem*. **2004**, 566, 111-121.
[25] H. J. Guadalupe, E. G. Ochoa, P. J. Maldonado-Rivas, J. Cruz, T. Pandiyan, *J. Electroana. Chem*. **2011**, 655, 164-172.

[26] J. Aljourani, M. A. Golozar, K. Raeissi, *Mater. Chem. Phys*. **2010**, 121, 320-325.
[27] M. Benabdellah, A. Tounsi, K. F. Khaled, B. Hammouti, *Arab. J. Chem*. **2011**, 4, 17-24.
[28] F. Zhang, Y. M. Tang, Z. Y. Cao, W. H. Jing, Z. L. Wu, Y. Z. Chen, *Corros. Sci*. **2012**, 61, 1-9.
[29] A. U. Ezeoke, O. G. Adeyemi, O. A. Akerele, N. O. Obi-Egbedi, *Int. J. Electrochem. Sci*. **2012**, 7, 534-553.
[30] W. Li, X. Zhao, F. L. Liu, B. Hou, *Corros. Sci.* **2008,** 50, 3261-3266.
[31] A. Chetouani, B. Hammouti, A. Aouniti, N. Benchat, T. Benhadda, *Prog. Org. Coat.* **2002,** 45, 373-378.
[32] G. N. Mu, X. H. Li, Q. Qu, J. Zhou, *Corros. Sci*. **2006**, 48, 445-459.
[33] R. A. Prabhu, A. V. Shhanbhag, T. V.Venkatesha, *J. Appl. Electrochem.* **2007**, 37, 491-497.
[34] I. Dehri, M. Ozcan, *Mater. Chem. Phys.* **2006**, 98, 316-323.
[35] A. Popova, *Corros. Sci.* **2007,** 49, 2144-2158.
[36] A. Popova, E. Sokolova, S. Raicheva, M. Chritov, *Corros. Sci*. **2003**, 45, 33-41.
[37] G. Quartarone, G. Moretti, A. Tassan, A. Zingales, *Mater. Corros.* **1994**, 45, 641-647.
[38] S. V. Ramesh, V. Adhikari, *Bull. Mater. Sci.* **2007**, 31, 699-711.
[39] A. Yurt, S. Ulutas, H. Dat, *Appl. Surf. Sci*. **2006**, 253, 919-925.
[40] H. Ashassi-Sorkhabi, M. Eshaghi, *Mater. Chem. Phys.* **2009,** 114, 267-271.
[41] F. Bentiss, M. Lebrini, M. Lagrenee, *Corros. Sci*. **2005,** 47, 2915-2931.
[42] S. F. Mertens, C. Xhoffer, B. C. Decooman, E. Temmerman, *Corrosion* **2000,** 53, 381-388.
[43] M. Behpour, S. M. Ghoreishi, N. Soltani, M. Salavati-Niasari, M. Hamadanian, A. Gandomi, *Corros. Sci.* **2008,** 50, 2172-2181.
[44] S. Martinez, M. M. Hucovic, *J. Appl. Electrochem.* **2003,** 33, 1137-1142.
[45] E. S. Ferreira, C. Giacomelli, F. C. Giacomelli, A. Spinelli, *Mater. Chem. Phys*., **2004**, 83, 129-134.
[46] M. Lebrini, F. Robert, C. Roos, *Int. J. Electrochem. Sci.* **2011**, 6, 847–859
[47] I. Ahamad, R. Prasad, M. A. Quraisi, *Corros. Sci.* **2010**, 52, 1472-1481.
[48] B. Trachli, M. Keddam, H. Takenouti, A. Srhiri, *Corros. Sci.* **2002**, 44, 997-1008.
[49] D. P. Schweinsberg, G. A. George, A. K. Nanayakkara, D. A. Steinert, *Corrosion Science*, **1988**, 28, 33- 42.
[50] A. S. Fouda, M. N. Mousa, F. I. Taha, A. I. Elneanaa, *Corros. Sci.* **1986,** 26, 719-726.
[51] M. K. Pavithra, T. V. Venkatesha, M. K. Punith Kumar, B. S. Shylesha, *Ind. Eng. Chem. Res.* **2013,** 52, 722–728.
[52] M.K.Pavithra, T.V.Venkatesha, K.Vathsala, K.O.Nayana, *Corros. Sci*., **2010,** 52, 3811–3819.